International Journal of Automotive Technology, Vol. 8, No. 6, pp. 781–790 (2007)

1229-9138/2007/037-13

EXPLORING THE FUEL ECONOMY POTENTIAL OF ISG HYBRID ELECTRIC VEHICLES THROUGH DYNAMIC PROGRAMMING

G.-Q. AO*, J.-X. QIANG, H. ZHONG, L. YANG and B. ZHUO

Institute of Automotive Electronic Technology, Shanghai Jiao Tong University, Shanghai 200030, China

(Received 3 April 2007; Revised 21 October 2007)

ABSTRACT–Hybrid electric vehicles (HEV) combined with more than one power sources have great potential to improve fuel economy and reduce pollutant emissions. The Integrated Starter Generator (ISG) HEV researched in this paper is a two energy sources vehicle, with a conventional internal combustion engine (ICE) and an energy storage system (batteries). In order to investigate the potential of diesel engine hybrid electric vehicles in fuel economy improvement and emissions reduction, a Dynamic Programming (DP) based supervisory controller is developed to allocate the power requirement between ICE and batteries with the objective of minimizing a weighted cost function over given drive cycles. A fuel-economy-only case and a fuel & emissions case can be achieved by changing specific weighting factors. The simulation results of the fuel-economy-only case show that there is a 45.1% fuel saving potential for this ISG HEV compared to a conventional transit bus. The test results present a 39.6% improvement in fuel economy which validates the simulation results. Compared to the fuel-economy-only case, the fuel & emissions case further reduces the pollutant emissions at a cost of 3.2% and 4.5% of fuel consumption with respect to the simulation and test result respectively.

KEY WORDS: ISG Hybrid electric vehicle, Supervisory controller, Dynamic programming, Cost function

1. INTRODUCTION

Research to increase fuel economy, decrease emissions and provide customer-affordable vehicles, without sacrificing performance, safety and reliability, has challenged the automotive industry for decades. Improving fuel economy is also a political issue, as it alleviates dependency on fuel import, and also reflects customer preferences for reducing vehicle operating cost.

HEVs are assumed to be one of the most promising alternatives to conventional engine-only powered vehicles. Furthermore, hybridization has been proved to be the most practical solution for providing customers with affordable, high fuel economy and less polluting vehicles. Some commercial hybrid vehicles have become available on the market, such as the Prius from Toyota and the Insight from Honda (Itagaki *et al.*, 2002; Kaoru *et al.*, 2000; Demirdöven and Deutch, 2004).

Generally, HEVs can be classified into three groups: series, parallel, and series parallel hybrid electric vehicles (Chan, 2002). Figure 1 shows a typical ISG parallel HEV that is the topic of this paper. In this architecture, both the ICE and electric motor are coupled to the drive shaft. Therefore, the propulsion power can be delivered by the ICE, by the electric motor or by both of these. The electric motor can act as a generator to charge the battery by absorbing power from the ICE when its output exceeds what is needed. The electric motor can also be used as a traction motor to provide extra power to assist the vehicle when the required power exceeds what the ICE can provide. Moreover, the HEV has the function of recovering kinetic energy through regenerative brakes which charges the battery during deceleration (Cho and Vaughan, 2006a, 2006b).

Because of the involvement of the electric motor, the HEV offers the possibility of providing total drive force in different ways which has significant influences on vehicle fuel economy, performance and drivability. The degree to which a hybrid vehicle is better than a conventional one depends heavily on how the drive force between ICE and electric motor is allocated. Over the past few decades, numerous control strategies have been conducted to address these issues.

Most control strategies for parallel HEV can be classified into three categories. The first is a rule-based control strategy, such as baseline control or rule-based control. They are real-time static optimization control strategies in which a set of rules are established to distribute the power between ICE and motor according to engineering intuition and simple analysis of components efficiency. These control strategies have been widely studied (Valerie

*Corresponding author. e-mail: aoguoqiang@sjtu.edu.cn

et al 2000; Baumann *et al.*, 2000).

The second is intelligent control strategy for estimation and control algorithm, such as rule-based fuzzy logic and ANN (Artificial Neural Nets). In these intelligent control strategies, expert knowledge is coded in the form of rules to allow a split of the power requirement between the ICE and the electric motor. Since the HEV control system is highly nonlinear with multiple objectives (driving ability, SOC sustaining, high fuel economy and low emissions), the fuzzy logic control strategy is widely used (Baumann *et al.*, 2000; Ao *et al.*, 2006; Pu *et al.*, 2005; Schouten *et al.*, 2002; Mohebbi *et al.*, 2005). The advantage of this fuzzy logic-based control strategy is that development of a fuzzy logic controller is less expensive and easier to understand since the rules are expressed in natural linguistic language.

The basic idea of the last strategy is global optimization such as mathematic programming (Galdi *et al.*, 2001), dynamic programming (Lin *et al.*, 2003; Perez *et al.*, 2006) and optimization algorithms based on a classical variation approach (Delprat *et al.*, 2002).

For the real-time control strategies mentioned above, there are no standard and systematic methods to transform the experts' knowledge, engineering intuition and experience into control strategy. Moreover, the expert's knowledge is often incomplete and episodic rather than systematic. Therefore, the global optimum result is not always guaranteed. Many trial-and-error-based tests are needed to tune and adjust the control variables or parameters.

The aim of this paper is to explore the fuel economy potential and find an optimal trajectory to achieve global minimum fuel consumption while minimizing emissions over given drive cycles. Dynamic programming provides a globally optimal solution to this constrained nonlinear programming problem. Since the achieved optimal results are independent of any control strategies by using the knowledge of past power used and future power demands, the optimal results represent the performance limit of this SOC sustaining ISG HEV. They can be used as benchmarks to assess and evaluate other control strategies. Moreover, some implemental rules or laws can be extracted from the results and applied to real-time control strategies, such as rule-based or fuzzy logic based control strategies (Lin *et al.*, 2003).

2. SYSTEM ARCHITECTURE AND MODEL

2.1. System Architecture

The ISG hybrid electric vehicle presented here is not a new one and is widely used in many hybrid vehicles, such as the Insight and the Civic sedan of Honda, the Chevrolet Silverado and the GMC Sierra full-size pickup of GM. Generally, ISG HEV is known as a mild parallel hybrid electric vehicle. In this configuration, an ISG motor is combined into the powertrain and located on the crankshaft between a compression-ignition direct-injection (CIDI) engine and a conventional clutch. This installation eliminates both the traditional starter motor and belt-driven alternator, as shown in Figure 1. The CIDI engine is downsized from 6 (7.8 L) to 4 (5.2 L) cylinders with the Engine Management System (EMS) from the Delphi Diesel System. The Battery Pack control Module (BPCM) is used to calculate the SOC and monitor the state of the battery packs. The Hybrid Control Unit (HCU) allocates the demanded power between the motor and ICE to satisfy the drive requirement.

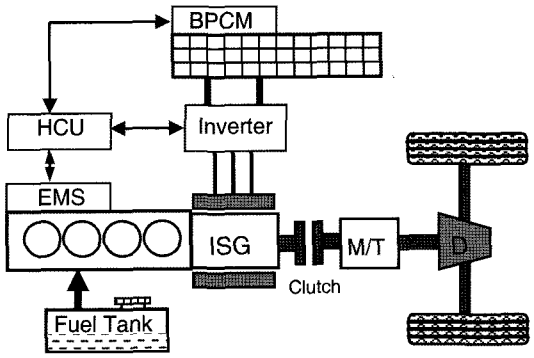

Figure 1. Schematic diagram of the ISG HEV.

The prototype ISG HEV developed in our institute is an 11-meter-long transit bus with a manual transmission. The basic components' specifications are listed in Table 1.

2.2. Components' Model of HEV

To avoid complexities and develop a time efficient simu-

Table 1. Basic specifications of vehicle.

Components items		Specifications
Vehicle	Curb weight	15000 Kg
	Rolling coefficient	0.014
	Aero-coefficient	0.79
	Frontal area	8 m^2
	Wheel radius	0.52 m
Engine	Type	CIDI
	Control system	Delphi Diesel System
	Max torque (Nm)	720@1300~1500 r/min
Motor	Type	PM brushless AC
	Max power & torque	60 kw & 400 Nm
Battery	Type	NiMH
	Capacity	40AH (312V)
Transmission	Gears	6.93/4.27/2.63/1.623/1.0
	Final drive	4.875

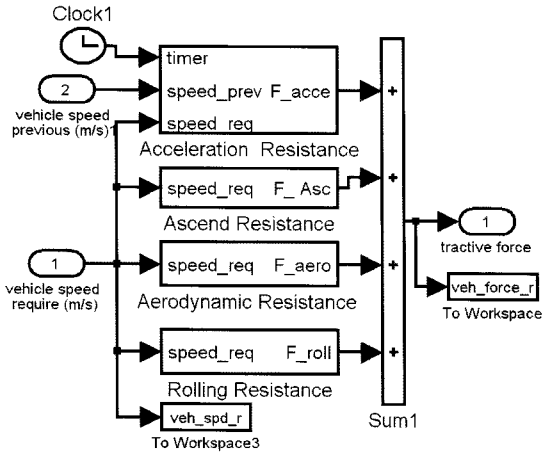

Figure 2. Drive force calculation model.

lation program, the vehicle is considered as a discrete dynamic system and simplified into five components which are sufficiently complex for evaluating the performance of the ISG HEV. All of the components are modeled in a Matlab/Simulink environment. These models are described below.

The prototype vehicle presented here is a city transit bus. The basic specifications are shown in Table 1. The vehicle subsystem includes the wheels/tires, transmission and body. The vehicle longitudinal dynamic model can be described as:

$$F_d=F_f+F_i+F_w+F_j \tag{1}$$

Where F_d is the total driving force requirement, F_f is the rolling resistance, F_i is the ascending resistance, F_W is the aerodynamic resistance and F_j is the acceleration resistance. The calculation diagram is shown in Figure 2.

For the engine model, the fuel consumption and emissions are static functions of two independent variables: engine speed and torque. The emissions maps of CO, HC, NOx and PM are obtained from a bench test. In this model, we assume that the engine is fully warmed. Hence, the engine temperature effect is not considered. The X-axis indicates engine speed of the steady state efficiency map of the engine shown in Figure 3.

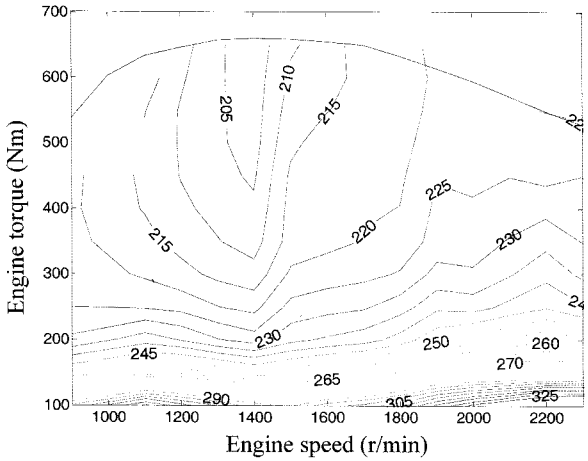

Figure 3. Engine efficiency map (test results of YC4112 CIDI engine).

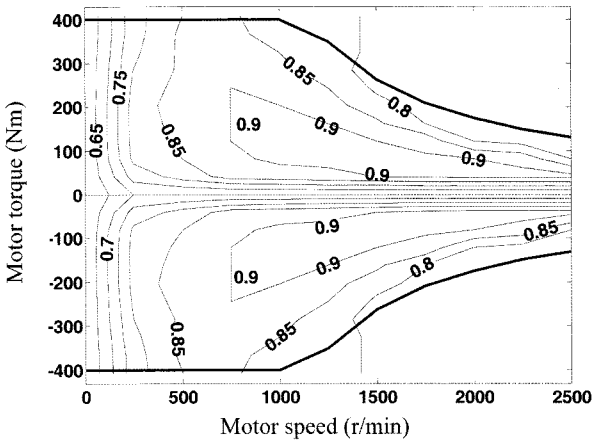

Figure 4. Efficiency map of motor (test results of PM motor specially designed for HEV).

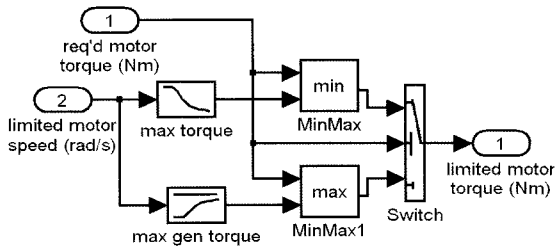

Figure 5. Torque output limits of motor.

The electric motor used in our prototype vehicle is a specially designed permanent magnet (PM) AC synchronous motor. The motor model is based on efficiency data which is a function of motor torque and speed. The X-axis is the motor speed as shown in Figure 4. Due to the battery and motor power limit, the final motor torque output is the minimum of the two components as shown in Figure 5.

Battery performance is a very complicated electrochemical process. For a battery model, the internal resistance model is used (Lin *et al.*, 2003).

The current can be calculated by the required electrical power and Kirchhoff's voltage law for the equivalent circuit

$$V_{oc}=V+R_{\text{int}}I \tag{2}$$

$$P=VI \tag{3}$$

$$P=T_m\omega_m\eta_m \tag{4}$$

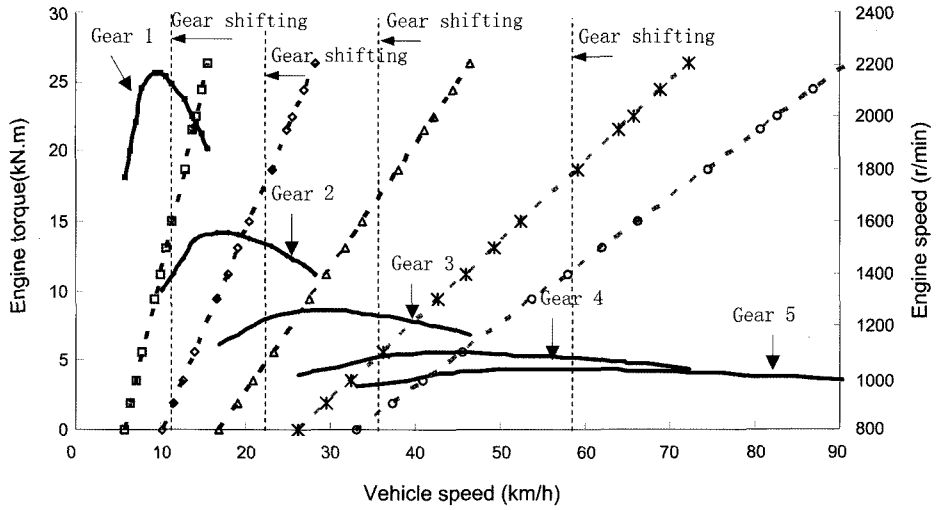

Figure 6. Gear shifting time and vehicle speed (dynamometer test results of the prototype vehicle).

Where V_{oc} is open-circuit voltage of battery, V is the terminal voltage, R_{int} is the internal resister of battery, I is the current in the circuit, P is required power from electric motor and T_m is motor torque, ω_m is motor speed and η_m is motor efficiency.

Combined with (2), (3), and (4), we have:

$$R_{int}I^2-V_{oc}I+P=0 \tag{5}$$

For the quadratic equation (5), there are two solutions. The larger current is not considered because the terminal voltage is under the low limit voltage to produce the same power which is not suited for the discharge characteristics of the NiMH battery.

Derived from (5), the current in or out of the battery can be expressed as:

$$I=\frac{V_{oc}-\sqrt{V_{oc}^2-4(R_{int}+R_t)T_m\omega_m\eta_e^{-\mathrm{sgn}(T_m)}}}{2(R_{int}+R_t)} \tag{6}$$

Where the R_t is load resister for the equivalent circuit.

SOC is computed assuming that the A-h capacity is constant. The max capacity can be denoted as C_{max} (rated 40AH in this paper), so the SOC can be calculated:

$$SOC_{k+1}=SOC_k-\frac{I\Delta t}{C_{max}} \tag{7}$$

Where Δt is the time duration of the current and C_{max} is the max capacity of the battery packs (in AH). Charge and discharge power are limited here in order to keep the bus voltage in a suitable range to prevent the battery from being overcharged or over-discharged.

In order to recreate the results of dynamometer testing more closely, a vehicle-speed dependent shift control was implemented. The gear shifting sequence is derived from the dynamometer test results shown in Figure 6. There are three groups of lines in Figure 6. The solid lines represent the maximum torque envelope on the wheel of the different gears at various vehicle speeds and torque space. The intersection points of the vertical dotted lines and X-axis indicate vehicle speed during gear shifting. The last group of lines represents the engine rotation speed of different gears on vehicle speed and engine rotation speed space.

3. PROBLEM STATEMENT

For this dual power sources hybrid electric vehicle, the energy flow diagram can be descried in Figure 7.

The power requirement at time t is denoted by $P_{req}(t)$ and it is assumed that it is the function of vehicle velocity and road slope.

$$P_{req}(t)=f_{veh}(v(t), h(t)) \tag{8}$$

Where the function $f_{veh}(v(t), h(t))$ is related to the rolling resistance, ascending resistance, aerodynamic resistance and acceleration resistance, as shown for equation (1). $v(t)$ is the vehicle speed requirement specified in the drive cycle and $h(t)$ is the road slope.

The fuel consumption of the engine at time t is denoted $Fuel(t)$ which is the function of engine power output $P_{ICE}(t)$. Thus, fuel consumption can be expressed as:

$$Fuel(t)=f_{ICE}(P_{ICE}(t)) \tag{9}$$

When engine power $P_{ICE}(t)$ is output to the drive shaft, the emissions generated at the same time is denoted by $CO(t)$, $HC(t)$, $NOx(t)$ and $PM(t)$ at time t. The calculation of fuel consumption and emissions is simplified as the static map of the engine.

For the battery packs, the SOC is calculated in relation to the battery capacity C_{max} and the power $P_{batt}(t)$ flowing into or out of the battery packs. It can be expressed as:

$$SOC(t)=1-\frac{f_{batt}(P_{batt}(t))}{C_{\max}} \tag{10}$$

Where $f_{batt}(P_{batt}(t))$ is the AH in or out of the battery.

In the motor diagram, the motor power $P_m(t)$ is determined by $SOC(t)$ and power requirement $P_{req}(t)$ at time t.

$$P_m(t)=f_m(SOC(t),\ P_{req}(t)) \tag{11}$$

$$=\begin{cases} P_{gen}(t) \text{ if } P_{req}(t)\le P_{gen\_th}\&SOC_{\min}<SOC(t)<SOC_{\max} \\ P_{acc}(t) \text{ if } P_{req}(t)\ge P_{gen\_th}\&SOC_{\min}<SOC(t)<SOC_{\max} \end{cases} \tag{12}$$

When braking or the required power $P_{req}(t)$ is lower than P_{gen_th}, threshold power for generation, the motor works as a generator to absorb kinetic energy or exceed engine power to charge the battery when SOC is low; When $P_{req}(t)$ is higher than P_{acc_th}, the threshold power for acceleration is assisted by additional power from the motor to drive the vehicle. A balance equation can be established naturally.

$$P_{req}(t)=P_{ICE}(t)+P_m(t) \tag{13}$$

For the given drive cycle, the total fuel consumption and emissions can be expressed:

$$Total\_f=\sum_{t=1}^{N} fuel(t) \tag{14}$$

$$Total\_emiss=\sum_{t=1}^{N}[CO(t)+HC(t)+NOx(t)+PM(t)] \tag{15}$$

As for the charge sustaining the hybrid electric vehicle, the battery is constrained to have the same amount of energy at the beginning and end of a cycle. So the net energy consumption of a battery over a given cycle can be zero.

$$E_{batt}=\sum_{t=1}^{N} P_{batt}(t)=0 \tag{16}$$

4. DP SOLUTION

For equation (13), the requirement power can be offered by the engine only, by the motor or by both of them. On the one side, if the required power delivered only by CIDI engine, the vehicle may miss the drive cycle and won't achieve optimal fuel economy. On the other side, if the vehicle is driven only by motor, this may deplete the battery and damage it. So the distribution of the power between the motor and engine while achieving satisfactory fuel consumption and emissions is important. The DP is selected to search an optimal trajectory to achieve global minimum fuel consumption and comprehensive optimal results over given drive cycles.

4.1. Bellman's Principle of Optimality

Dynamic programming is based on Bellman's Principle of Optimality (Bellman *et al.*, 1962; Bertsekas *et al.*, 2002; Bertsekas *et al.*, 2005). This principle states that: "An optimal policy or a set of decisions has the property that whatever the initial state and optimal first decision may be, the remaining decisions constitute an optimal policy with regard to the state resulting from the first decision." (Bellman *et al.*, 1962). It can be expressed as:

$$P^*_{1,n}=\{u^*_1,u^*_2,\ldots,u^*_n\} \tag{17}$$

Where $u^*_1,u^*_2,\ldots,u^*_n$ are the decisions or control variables. $P^*_{1,n}$ is a multi-stage optimal policy for the discrete-time deterministic dynamic optimization problem which minimizes the weighted cost function J.

$$J=\sum_{i=1}^{N} L(x_i,u_i) \tag{18}$$

Where

$$x_{i+1}=f(x_i,u_i),\ i=1,2,\ldots,N$$

Subjected to

$$x\in X(i)\subset R^n,\ u\in U(x_i,i)\subset R^m$$

Where x_{i+1} is the state vector of the system, u_i is the control variables vector, i is the stage, f is the transition function, R^n, R^m are the state space of $X(i)$ and control variable space of $U(x_i,\ i)$ respectively, J is the cost function and $L(x_i,\ u_i)$ is the stage cost at i stage. For the HEV, the cost function can be presented:

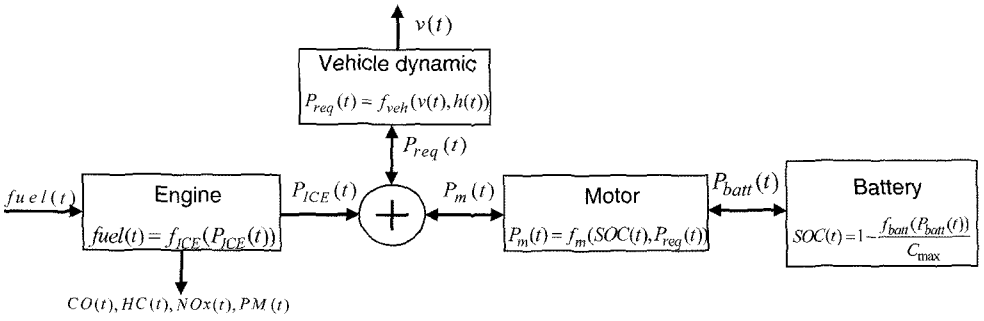

Figure 7. Energy flow diagram of ISG HEV.

$$J=\sum_{i=1}^{N} L(x_i,u_i)$$

$$=\sum_{i=1}^{N} [fuel(x_i,u_i)+W_1CO(x_i,u_i) \quad (19)$$

$$+W_2HC(x_i,u_i)+W_3NOx(x_i,u_i)+W_4PM(x_i,u_i)]$$

Where $fuel(x_i,u_i)$ is the fuel consumption at the i stage, $CO(x_i,u_i)$, $HC(x_i,u_i)$, $NOx(x_i,u_i)$ and $PM(x_i,u_i)$ are the emissions at i stage. W_1, W_2, W_3 and W_4 are positive weighting factors of CO, HC, NOx and PM respectively.

During drive cycles, the following constraints should be imposed.

$$\omega_{ICE\_min} \le \omega_{ICE}(i) \le \omega_{ICE\_max} \quad (20)$$

$$T_{ICE\_min} \le T_{ICE}(i) \le T_{ICE\_max} \quad (21)$$

$$\omega_{m\_min} \le \omega_m(i) \le \omega_{m\_max} \quad (22)$$

$$T_{m\_min} \le T_{ICE}(i) \le T_{m\_max} \quad (23)$$

$$SOC_{min} \le SOC(i) \le SOC_{max} \quad (24)$$

Where ω_{ICE} is the ICE speed, T_{ICE} is the ICE torque, T_m is the motor torque, SOC is the state charge of the battery. SOC_{min} and SOC_{max} are set to 0.3 and 0.8 respectively. Discharge is not allowed when the SOC is lower than SOC_{min} and charge is not allowed when the SOC reaches SOC_{max}. This function is conducted by constraining the state variable SOC within 0.3 to 0.8.

For this ISG HEV, the motor is directly coupled to the crankshaft, so the motor speed and the ICE speed is the same:

$$\omega_{ICE}=\omega_m \quad (25)$$

In formulation (19), there are no constraints on terminal $SOC(N)$, and the optimization algorithm tends to deplete the battery to achieve minimal fuel consumption. In order to prevent the batteries from depleting, a penalization function is needed. The difference between objective $SOC(obj)$ and final $SOC(N)$ is used (Lin *et al.*, 2003). The SOC calculation is based on the accumulated current approach. Therefore, the current flowing in or out of the battery can be used as the penalization term to achieve a SOC sustaining optimum trajectory. So the cost function can be expressed as:

$$J=\sum_{i=1}^{N} [fuel(x_i,u_i)+W_1CO(x_i,u_i)+W_2HC(x_i,u_i) \quad (26)$$

$$+W_3NOx(x_i,u_i)+W_4PM(x_i,u_i)+W_5I(x_i,u_i)]$$

Where $I(x_i,u_i, i)$ is the current of battery at i stage and W_5 is the battery current weighting factor.

4.2. DP Algorithm Implementation

Dynamic programming based on Bellman's Principle of Optimality is a powerful numerical technique that can be applied for any dynamic optimization problem. In this method, serial control decisions are made during every stage with the objective of finding a minimal pathway (Bellman and Dreyfus, 1962).

In this paper, a backward dynamic program with interpolation is used to solve the optimization solutions backwards. In this way, the last stage is solved first and then extended to the last two stages, the last three stages,..., etc., until the entire problem is solved. In this backward method, the engine power $P_{ICE}(t)$ is chosen as the control variable and the SOC is selected as state variable x, shown in Figure 8. The pseudo codes of this backward DP method are shown in Figure 9.

For the first step: Solve the last stage i=N

$$J(N)=\min_{u(N)} L(x_N,u_N,N) \quad (27)$$

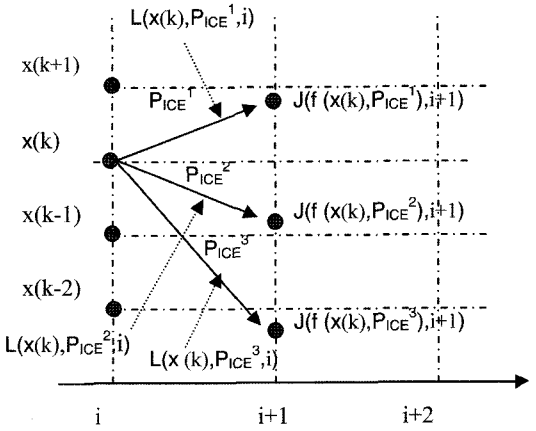

Figure 8. Backward DP algorithm with interpolation.

```
Initialize J(x, i) = ∞ , ∀ x∈X(i), ∀i
Evaluate J(x, N), ∀ x∈X(N)
For all the stages i= N – 1 to 1
  For all the quantified states xk(i) ∈X(i)
    For all the admissible decisions
      uj(i) ∈U[xk(i), i]
       Evaluate the transition function f (xk,uj,i)
       If g (xk, uj, i) ∈X(i+1)
          Interpolate J(f(xk, uj, i), i+1)
        If L(xk, uj, i) +J(f(xk, uj, i),i+1)<J(xk,i)
            J(xk, i)= L(xk,uj,i) +J(f (xk, uj, i),i+1)
            u* (xk, i)= uj
          End if
        End if
      End for
    End for
End for
```

Figure 9. Pseudo code of the backward dynamic program with interpolation.

$$L(x_N,u_N,N) = fuel(x_N,u_N)+W_1CO(x_N,u_N)+W_2HC(x_N,u_N) + W_3NOx(x_N,u_N)+W_4PM(x_N,u_N)+W_5I(x_N,u_N) \quad (28)$$

For the generic induction step i:
For $1 \le i \le N$ $(i = 1, 2, 3, \ldots, \text{N-1})$

$$J(i)=\min_{u(i)} J(i+1)+L(x_i,u_i,i) \quad (29)$$

Where

$$L(x_i,u_i,i) = fuel(x_i,u_i)+W_1CO(x_i,u_i)+W_2HC(x_i,u_i) + W_3NOx(x_i,u_i)+W_4PM(x_i,u_i)+W_5I(x_i,u_i) \quad (30)$$

During our simulation implementation, $J(i)$ are calculated to search for the optimal pathway at each sample time. To ensure strictly that all constraints listed in (20)~(24) are not violated, the constraints are computed simultaneously.

5. DP SIMULATION RESULTS

In previous work, the longitudinal dynamics and components of this prototype HEV has been modeled in Matlab/Simulink and validated through road and bench tests. The specifications of the prototype HEV are shown in Table1.

The dynamic programming controller has been embedded into this quasi-static vehicle model shown in Figure 10. This optimal algorithm will search a series of control variables to minimize the weighted cost function consisting of fuel consumption and emissions while constraining the SOC sustainable. A SOC sustainable vehicle means that the SOC at the end of the cycle is (almost) the same as the beginning. The largest SOC difference for the simulations and tests in this paper is 0.13%, which is smaller than the usually used tolerance of 0.5% which indicates that the simulation and test results are reliable (SAE J1711, 1999).

This section presents simulation and test results of the conventional transit bus and the sustaining ISG hybrid vehicle. For the HEV, the fuel-economy-only case and fuel & emissions case can be achieved by changing the specific weighting factors. According to the two cases of optimal results presented in this paper, real road tests were conducted. The test results are consistent with the simulation shown in Table 3.

5.1. Charge-Sustaining Strategy

ISG HEV is a mild hybrid electric vehicle with a relatively small motor and battery. So a charge sustaining the control strategy is needed. By changing the weighting factor of the current weighting factor W_5, charge sustaining target can be achieved.

Figure 11 presents SOC histories of three cases with three different weighting factors. In these cases, the initial $SOC(1)$ are all set to 0.7, while the terminal $SOC(N)$ are different from different weighting factors W_5. The higher $SOC(N)$ is with the higher weighting factor. When W_5 is set to 1400, the $SOC(N)$ is 0.701 which is the selected weighting factor for the charge sustaining strategy. Table 2 lists the terminal SOC of the three cases with different weighting factors.

Figure 12 presents the simulation results for the sustaining strategy over the China Urban Drive Cycle (CUDC)

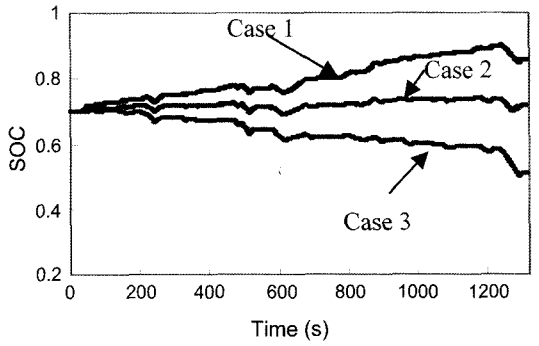

Figure 11. SOC history with different weighting factors.

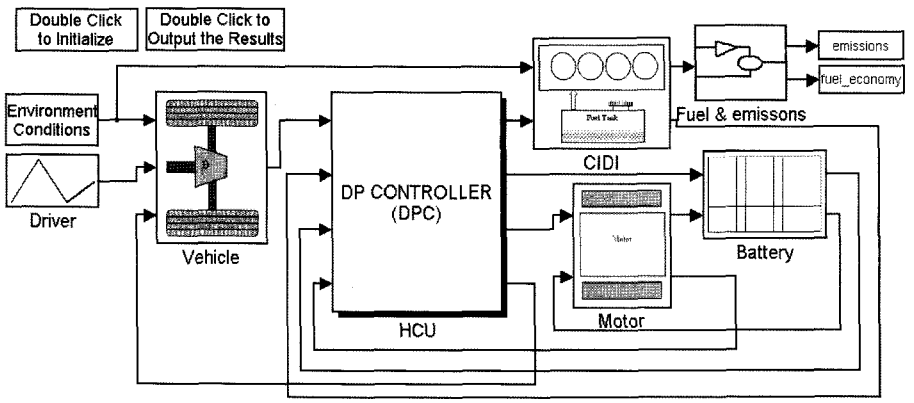

Figure 10. Simulation model in Matlab/Simulink.

Table 2. *SOC(N)* with different weighting factors.

Case	Weighting factors	*SOC (N)*
1	W_1=1 W_2=W_3=W_4=0 W_5=1200	0.85
2	W_1=1 W_2=W_3=W_4=0 W_5=1400	0.701
3	W_1=1 W_2=W_3=W_4=0 W_5=1500	0.51

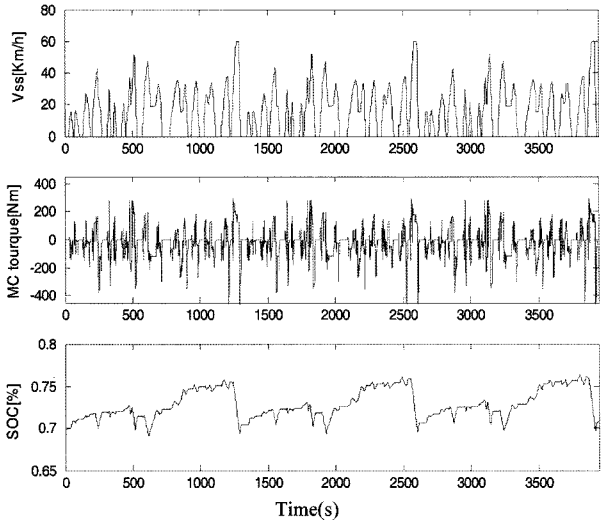

Figure 12. CUDC and SOC history.

(CNASTC, 2005) in which the SOC is maintained over a long time horizon simulation (3 CUDC). The X-axis indicates the simulation time shown in Figure 12.

5.2. Fuel Economy Optimization Results

In order to evaluate the dynamic programming, several drive cycles were tested including typical urban and highway cycles.

The relative size of the weighting factors is decided by comparing the mean values of engine fuel rate, emissions flow rate and battery current. In the fuel-economy-only case, the weighting factors W_1, W_2, W_3 and W_4 are set to zero, and W_5 is set to 1400 for the SOC sustaining purpose.

Figure 13 and Figure 14 present the fuel-economy-only case optimizing results over the driving cycle of CUDC and ECE+EUDC. The Curves of the cycle velocity (Vss), the total torque requirement, the optimal trajectory of ICE torque, MC torque and the SOC history are all presented. The X-axis indicates the simulation time. For all simulation results, the SOC was corrected within –0.13% to 0.13%.

Table 3 presents the fuel economy and emissions of the simulation and test results over CUDC. Also, the conventional transit bus fuel economy and emissions are given for comparison. For the simulation results, there is a 45.1% fuel saving potential compared to the conventional transit bus. The real road test achieved 39.6% fuel saving according to the optimal results presented in this paper compared to the conventional transit bus. The difference between the test and simulation result is due to two conditions. First, it is difficult exactly to control the CIDI engine and motor on the optimal trajectory presented in this paper. Secondly, the simulation results are based on

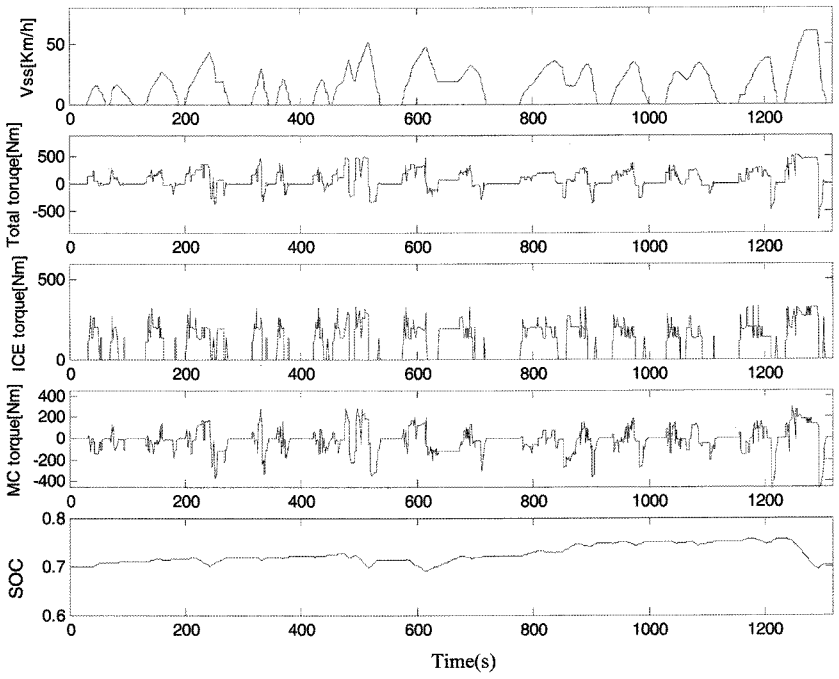

Figure 13. Simulation results over CUDC.

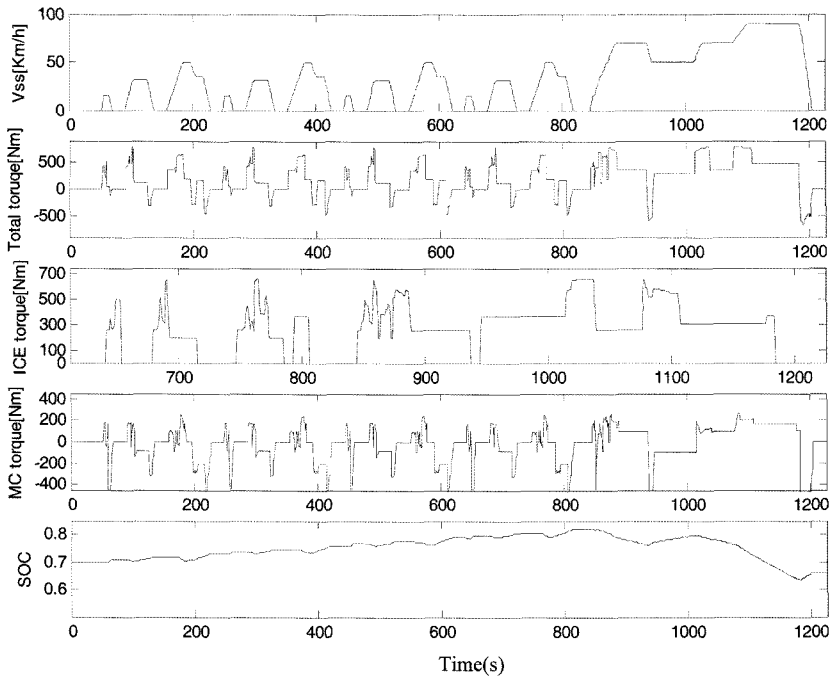

Figure 14. Simulation results over ECE+EUDC.

Table 3. Simulation and test results for the fuel-economy-only case and fuel & emissions case.

Cases	Fuel/(L/100 km)		CO (g/km)		HC (g/km)		NOx (g/km)		PM (g/km)	
	Simula-tion	Test results	Simula-tion	Test results	Simula-tion	Test results	Simula-tion	Test results	Simula-tion	Test results
Conventional bus	45	42.7	0.156	0.149	0.138	0.135	0.435	0.454	0.184	0.193
Fuel-economy-only	24.7	25.8	0.127	0.134	0.094	0.101	0.38	0.41	0.144	0.152
Fuel & emissions	25.5	27.1	0.109	0.12	0.085	0.093	0.303	0.332	0.119	0.128

Emissions: hydrocarbons (HC), carbon monoxide (CO), oxides of nitrogen (NOx) and particulate matter (PM).
Fuel-economy-only case: $W_1=W_2=W_3=W_4=0$, $W_5=1400$; fuel & emissions case: $W_1=W_2=100$ $W_3=W_4=1000$ $W_5=1350$

fuel and motor steady state efficiency maps, while the real road test results originate from the transient operation condition of the CIDI engine and motor. Emissions are also reduced significantly mainly due to the HEV controller which automatically turns the engine off when the vehicle comes to a stop and restarts it when the driver depresses the accelerator pedal. This "stop-go" mode can save fuel and reduce CO and HC greatly. Moreover, the motor will deliver extra mechanical power when the vehicle is in high load driving conditions, which will reduce the NOx and PM greatly. Furthermore, the function of regenerative braking can absorb the braking energy to charge the battery during deceleration to improve fuel economy.

5.3. Fuel Economy and Emissions Trade-off

To further reduce exhaust emissions, the weighting factors related to emissions are raised to achieve fuel & emissions optimization results. In the fuel & emissions case, W_1 and W_2 are set at 100, W_3 and W_4 are set at 1000 and the W_5 is set at 1350 for SOC sustaining purposes. The DP controller will search the most efficient operating points to minimize the weighted cost function while satisfying the power demand. For the simulation of the fuel & emissions case, the NOx, PM, CO and HC are 20.5%, 17.6%, 14.2% and 9.6% lower respectively, at the cost of a 3.2% fuel consumption increase compared to the fuel-economy-only case. The real road test results show that there is a 19%, 15.8%, 10.4% and 7.9% decrease in NOx, PM, CO and HC respectively with a 4.5% fuel consumption increase compared to the fuel-economy-only case. Because of the relatively smaller weighting factors ($W_1=W_2=100$) for the CO and HC, the reduction of CO and HC emissions is smaller than the NOx and PM emissions, which validates the simulation results.

6. CONCLUSIONS

A dynamic programming algorithm can be used to explore the fuel economy potential with the constraints of SOC sustaining and without sacrificing the drivability. The DP controller, embedded into the ISG HEV model, distributes the traction power between the ICE and motor to acquire an optimal trajectory by minimizing the weighted cost function over given drive cycles. Small changes in specific weighting factors of the cost function emphasize either fuel economy optimization or a reduction in emissions. The optimal results of the fuel-economy-only case and the fuel & emissions case were analyzed and tested on the road over CUDC. The test results showed that the optimal results based on the dynamic program can improve fuel economy by more than 39.6% when tuned for a fuel-economy-only case. In the fuel & emissions case, a significant emission reduction could be achieved with a small decrease in fuel economy.

ACKNOWLEDGEMENT–This work was founded by The Ministry of Science and Technology of the People's Republic of China (973) under contract No. 2007CB209707. Also, the authors want to express appreciation to all the students and faculties in Institute of Automotive Electronic Technology of Shanghai Jiao Tong University for their contributions.

REFERENCES

Ao, G. Q., Zhong, H., Yang, L., Qiang, J. X., and Zhuo, B. (2006). Fuzzy logic based control for ISG hybrid electric vehicle. *Intelligent Systems Design and Applications, ISDA '06. 6th Int.Conf.*, **1**, 274–279.

Baumann, B. M., Washington, G., Glenn, B. C. and Rizzoni, G. (2000). Mechatronic design and control of hybrid electric vehicles. *IEEE/ASME Trans. Mechatronics* **5**, **1**, 58–72.

Bellman, R. E. and Dreyfus, S. E. (1962). *Applied Dynamic Programming.* Princeton University Press. New Jersey.

Bertsekas, D. (2002). *Lecture Slides on Dynamic Programming.* Based on Lectures Given at MIT. Cambridge. Massachusetts.

Bertsekas, D. P. (2005). *Dynamic Programming and Optimal Control.* 3rd edn. Athena Scientific. New Hampshire.

Chan, C. C. (2002). The state of the art of electric and hybrid vehicles. *Proc. IEEE* **90**, **2**, 247–275.

Cho, B. and Vaughan, N. D. (2006a). Dynamic simulation model of a hybrid powertrain and controller using co-simulation Part I: Powertrain modeling. *Int. J. Automotive Technology* **7**, **4**, 459–468.

Cho, B. and Vaughan, N. D. (2006b). Dynamic simulation model of a hybrid powertrain and controller using co-simulation-Part II: Control strategy. *Int. J. Automotive Technology* **7**, **7**, 785–793.

CNASTC (2005). Test methods for energy consumption of high-duty hybrid electric vehicles. *Chinese National Automobile Standardization Technology Committee.* Standard No: GB/T 19754-2005.

Delprat, S., Guerra, T. M. and Rimaux, J. (2002). Control strategies for hybrid vehicles optimal control. *Proc. 56th IEEE Vehicular Technology Conf.*, **3**, Vancouver, Canada, 1681–1685.

Demirdöven, N. and Deutch, J. (2004). Hybrid cars now, fuel cell cars later. *Science*, **305**, 974.

Galdi, V., Ippolito, L., Piccolo, A. and Vaccaro, A. (2001). Multi-objective optimization for fuel economy and emissions of HEV using the goal-attainment method. *Proc. 18th Int. Electric Vehicle Symp.*, Berlin, Germany.

Itagaki, K., Teratani, T., Kuramochi, K., Nakamura, S., Tachibana, T., Nakao, H. and Kamijo, Y. (2002). Development of the Toyota mild-hybrid system (THS-M). *SAE Paper No.* 2002-01-0990.

Johnson, V. H., Wipke, K. B., and Rausen, D. J. (2000). HEV control strategy for real-time optimization of fuel economy and emissions. *SAE Paper No.* 2000-01-1543.

Kaoru, A., Shigetaka, K., Shigemasa, K., Hiromitsu, S. and Yoshio, Y. (2000). Development of integrated motor assist hybrid system: development of the 'Insight', a personal hybrid coupe. *SAE Paper No.* 2000-01-2216, Government/Industry Meeting, Washington, D.C., USA.

Lin, C. C., Zoran, F., Wang, Y. S., Loucas, L., Peng, H., Assanis, De., and Stein, J. (2001). Integrated, feed-forward hybrid electric vehicle simulation in SIMULINK and its use for power management studies. *SAE Paper No.* 2001-01-1334.

Lin, C. C., Peng, H., Grizzle, J. W. and Kang, J. M. (2003). Power management strategy for a parallel hybrid electric truck. *IEEE Tran. Control Systems Technology* **11**, **6**, 839–849.

Mohebbi, M., Charkhgard, M. and Farrokhi, M. (2005). Optimal neuro-fuzzy control of parallel hybrid electric vehicles. *Vehicle Power and Propulsion. IEEE Conf.* **7**, **9**, 26–30.

Perez, L. V., Bossio, G. R., Moitre, D. and Garcia, G. (2006). Optimization of power management in an hybrid electric vehicle using dynamic programming. *Mathematics and Computers in Simulation* **73**, 1–4, 244–254.

Pu, J. H., Yin, C. L. and Zhang, J. W. (2005). Fuzzy torque control strategy for parallel hybrid electric vehicles. *Int. J. Automotive Technology* **6**, **5**, 529–536.

SAE J1711 (1999). *Recommended Practice for Measuring the Exhaust Emissions and Fuel Economy of Hybrid-Electric Vehicles.* SAE Int..

Schouten, N. J., Salman, M. A. and Kheir, N. A. (2002). Fuzzy logic control for parallel hybrid vehicles. *IEEE Tran. Control System Technology* **10**, **3**, 460–468.